Psychoneuroendocrinology 110 (2019) 104441

Contents lists available at ScienceDirect

Psychoneuroendocrinology

journal homepage: www.elsevier.com/locate/psyneuen

# Sex-specific effects of prenatal valproic acid exposure on sociability and neuroinflammation: Relevance for susceptibility and resilience in autism

Nadia Kazlauskas[a,b], Araceli Seiffe[a,b], Marcos Campolongo[a,b], Cecilia Zappala[a,b], Amaicha Mara Depino[a,b,*]

[a] Universidad de Buenos Aires, Facultad de Ciencias Exactas y Naturales, Departamento de Fisiología, Biología Molecular y Celular, C1428EHA, Buenos Aires, Argentina
[b] CONICET-Universidad de Buenos Aires, Instituto de Fisiología, Biología Molecular y Neurociencias (IFIBYNE), Buenos Aires, Argentina

ARTICLE INFO

*Keywords:*
Autism spectrum disorders
Valproic acid
Sex-specific effects
Sociability
Neuroinflammation

ABSTRACT

Autism spectrum disorder (ASD) is a group of neurodevelopmental disorders with an incidence four times higher in boys than in girls. By analyzing the effect of sex in a mouse model of ASD, we were able to identify immune alterations that could underlie this sex bias.

Pregnant mice were injected subcutaneously with 600 mg/kg of valproic acid (VPA) or saline at gestational day 12.5. Their male and female offspring were evaluated in a social interaction test at adulthood, and only male VPA mice showed reduced sociability levels and a lack of preference for the social stimulus over a novel object. We then analyzed the corticosterone (CORT) response to an inflammatory stimulus, as a measure of the hypothalamus-pituitary-adrenal (HPA) function, and the neuroinflammatory state in adult and young animals. Adult VPA males exhibited increased basal CORT levels, while VPA females showed levels comparable to controls. As male mice showed a blunted CORT response at PD21 when compared to female mice, we propose that this early dimorphism could explain the different effects of VPA on HPA function. In addition, prenatal VPA exposure resulted in altered astroglial and microglial cell density levels in the cerebellum and dentate gyrus of adult mice. These neuroinflammatory effects were more pronounced in females than males, and appeared at early developmental stages. Hence, these postnatal glial density differences could underlie the behavioral alterations observed in adulthood, when only males show a social deficit.

Our work contributes to the understanding of biological mechanisms affected by VPA on male and female rodents and shed light on the study of possible resilience mechanisms in the female population and/or susceptibility to ASD in boys.

## 1. Introduction

Autism spectrum disorder (ASD) is a group of neurodevelopmental pathologies characterized by impairments in social interaction and communication, and also by the presence of repetitive or stereotyped behaviors and interests (American Psychiatric Association, 2013). Recently, the number of diagnosed children has increased and reached values up to 1 in 38 (Kim et al., 2011; Zablotsky et al., 2015). One of the most conspicuous biological factors associated with these disorders is the sex difference: more than 80% of the children diagnosed with ASD are boys (Centers for Disease Control and Prevention, 2009). Authors have proposed that this bias is due to the altered expression of genes located in sex chromosomes or abnormal exposure to sex hormones [reviewed in (Schaafsma and Pfaff, 2014)]. Here we tested an alternative hypothesis: that an environmental factor associated with ASD (prenatal exposure to VPA) can differentially affect male and female subjects. This can be interpreted also as a two-hit hypothesis, similar to the three-hit model were a genetic factor (Cntnap2 expression), an environmental factor (maternal immune activation) and sex are combined to modulate social recognition (Schaafsma et al., 2017).

In children, prenatal exposure to the anticonvulsant valproic acid (VPA) can increase up to 10-fold the risk to develop ASD (Rasalam et al., 2005). Supported by this clinical evidence, the prenatal administration of VPA at gestational day (GD) 12.5 has been extensively used

*Abbreviations:* ASD, autism spectrum disorders; CORT, corticosterone; DG, dentate gyrus; GD, gestational day; HPA, hypothalamus-pituitary-adrenal; LPS, lipopolysaccharides; PD, postnatal day; VPA, valproic acid

* Corresponding author at: Instituto de Fisiología, Biología Molecular y Neurociencias (IFIBYNE), CONICET-UBA. Int. Guiraldes 2160, Ciudad Universitaria, Edificio IFIBYNE, C1428EHA, Buenos Aires, Argentina.
*E-mail address:* adepino@conicet.gov.ar (A.M. Depino).

https://doi.org/10.1016/j.psyneuen.2019.104441
Received 24 May 2019; Received in revised form 9 September 2019; Accepted 10 September 2019

as a rodent model of ASD. VPA animals show a reduction in sociability (Lucchina and Depino, 2014) and increased stereotyped behaviors (Schneider et al., 2008), in addition these animals present several cellular and molecular alterations also observed in ASD individuals (de Theije et al., 2014; Lucchina and Depino, 2014). Interestingly, decreased sociability, increased repetitive behaviors, and anxiety-related behaviors have been observed in VPA males (Kim et al., 2013; Lucchina and Depino, 2014; Schneider et al., 2008), but not in females prenatally exposed to VPA (Kataoka et al., 2013; Kim et al., 2013; Schneider et al., 2008). We (Kazlauskas et al., 2016; Lucchina and Depino, 2014) and others (Schneider et al., 2008) have also found immunological alterations in the VPA model of ASD, similarly to immune alterations observed in people with ASD (Vargas et al., 2005). Some of these immunological alterations also show differences in their expression in male and female animals (Schneider et al., 2008). It has been reported that children with ASD have increased cortisol responses to environmental and social stressors (Corbett et al., 2006; Spratt et al., 2012). This augmented response could result from altered perception and/or interpretation of stressful stimuli, or a consequence of altered hypothalamus-pituitary-adrenal (HPA) axis function. In turn, cortisol can affect immune function. We have previously shown a normal corticosterone (CORT) response to an intraperitoneal LPS challenge in young VPA females [from postnatal day 7 to 42; (Kazlauskas et al., 2016)], but an exacerbated CORT response in adult VPA males in a C57BL/6 J x Balb/c F1 (Lucchina and Depino, 2014).

Due to unbalanced incidence of ASD in males to females (Fombonne, 2003), animal studies tend to be carried out mainly in male subjects. Our aim here was to characterize the effects of VPA on male and female mice, directly testing the effect of sex on social interaction, the corticosterone (CORT) basal levels and in response to an inflammatory stimulus, and the neuroinflammatory state. Moreover, we performed these experiments on adult mice and at postnatal day (PD) 21, a critical age regarding neuroinflammatory alterations in animals prenatally exposed to VPA (Kazlauskas et al., 2016) when social deficits can already be observed (Campolongo et al., 2018). We reasoned that if CORT response and neuroinflammation contribute to VPA effects on sociability, they should be differentially expressed in males and females. In addition, by studying young and adult animals we expected to evidence specific neuroimmune alterations that could mediate the development and/or the manifestation of social behavior. We consider that studying female subjects in animal model research can help understanding the particularities of ASD symptoms observed in girls, and also give evidence on possible resilience mechanisms in the female population.

## 2. Material and methods

### 2.1. Animals

Outbred CrlFcen:CF1 female and male adult mice were obtained from the animal house at the Faculty of Exact and Natural Sciences, University of Buenos Aires (Buenos Aires, Argentina). We chose this outbred stock because 1) these animals have better breeding performance than inbred strains, 2) they show reliable intermediate levels of social behavior, allowing the detection of increases and decreases in the behavioral parameters evaluated, and 3) VPA does not alter litter size nor gestation time in CF1 dams. The VPA model was generated as previously described (Campolongo et al., 2018; Kazlauskas et al., 2016). 8–10 week-old male mice were mated with nulliparous adult female mice. Females were controlled every morning, and the day when a vaginal plug was detected was considered the gestational day (GD) 0.5. On GD12.5, pregnant mice were randomly injected subcutaneously with either 600 mg/kg of valproic acid sodium salt (VPA; Sigma, St. Louis, MO,USA) in 0.9% NaCl or with vehicle (Veh), and housed individually. The parturition day was registered as postnatal day 0 (PD0), and the cage bedding was not changed during the first postnatal week to avoid nest alterations. On PD21, litters were weaned in cages containing 4–5 animals of the same sex and treatment. Offspring belonging to the same treatment group were mixed at weaning to reduce the litter + cage effect. Four cohorts of animals were used for the experiments: the first and second cohorts were used for social behavior testing, immunofluorescence and radioimmunoassay (RIA) studies in adult animals. Both of these cohorts were composed of 8 VPA and 8 Veh litters. The third cohort was used for PD21 immunofluorescence and RIA analyses and consisted of 5 VPA and 5 Veh litters. The fourth cohort was used for RT-PCR analysis. In each litter, 2–3 animals per sex were randomly chosen for behavioral testing. For all other analyses, one female and one male were randomly chosen from each litter and assigned to adult or PD21 RIA, immunofluorescence or RT-PCR analyses. All animals were housed on a 12:12 light:dark cycle and 18–22 °C temperature, with food and water ad libitum. All animal procedures were performed according to the regulations for the use of laboratory animals of the National Institute of Health (Washington, DC, USA) and approved by the institutional animal care and use committee of the Faculty of Exact and Natural Sciences, University of Buenos Aires (CICUAL Protocol Nr. 6/2012).

### 2.2. Sociability testing

The social interaction test was performed on 8–10 weeks old mice during the light period (between 9:00 and 16:00 h), as previously described (Campolongo et al., 2018). We tested 15 Veh males, 18 VPA males, 12 Veh females and 11 VPA females. Briefly, the test consists of a habituation period of 5 min, when the mouse is allowed to freely explore the experimental arena, followed by a testing period of 10 min. Between both phases, a juvenile mouse (21–28 days old) subject was placed in one of the cylinders, and a small object was placed in the opposite cylinder as a control. The compartment with the juvenile mouse was named “social side”, and the compartment with the object “non social side”. The social side was randomly chosen. After testing, each mouse was identified and placed in a holding cage until all animals in a cage were tested. The testing order of each cage was randomly established. Each apparatus was cleaned with 20% ethanol solution between sessions to eliminate odors and waste. Male and female mice were tested on different days, and the sex of the social stimulus and the experimental mouse was matched to prevent sexual or aggressive interactions. The trials were recorded and the time the subject spent sniffing the social stimulus was quantified manually using a video-tracking system (ANY-maze, Stoelting, IL, USA). All manual scoring was performed by an experimenter (N.K.) blinded to treatment groups. Sociability was calculated as the percentage of time the animal spent sniffing the social stimulus divided by the total time it spent sniffing the cylinders (social + non social).

### 2.3. Histological analyses

#### 2.3.1. Tissue preparation

Five animals per experimental group were randomly chosen from the first and second cohorts and sacrificed one week after social interaction test (between PD67 and PD77) for histological analyses. From the third cohort, five animals per experimental group were sacrificed at weaning (PD21). Animals were deeply anesthetized (i.p. 80 mg/kg ketamine chlorhydrate and 8 mg/kg xylazine), and transcardially perfused with heparinized saline followed by cold 4% paraformaldehyde (PFA) in 0.1 M phosphate buffer (PB), pH = 7.2. The brains were removed and placed in PFA for 4 h at 4 °C and then cryopreserved in a 30% sucrose solution in PB at 4 °C. All brains were frozen with isopentane and 40 µm sections were obtained with a cryostat (Leica Biosystems, Nussloch, Germany) and stored at − 20 °C. The brains were sectioned in the coronal plane, whereas the cerebella were sectioned in the sagittal plane.

#### 2.3.2. Astroglia and microglia quantification

Astroglial and microglial analyses were performed as previously described (Kazlauskas et al., 2016), using the primary antibody rabbit anti-glial fibrillary protein (GFAP; 1:700, DAKO, Glostrup, Denmark) for astroglial analysis and rabbit anti-Iba1 primary antibody (WAKO, Osaka, Japan) for microglial analysis. We classified microglial cells according to their morphology as previously described (Kazlauskas et al., 2016): Ramified: rod-shape cells with long and thin processes; Hypertrophic: ovoid cells with short and thick processes: and Ameboid/Round: macrophage-like round cells. Confocal microscopy photographs were obtained with a Confocal Olympus FV300/BX61 microscope under 400× magnification. Z stack images were taken 1 μm apart and analyzed with Olympus Fluoview 2.0 viewer. For each marker, between 3 and 5 sections per animal were analyzed to obtain the cellular density in each brain structure. The dorsal hippocampus (bregma -1.46 mm to -2.46 mm) and the vermis of cerebellum (lateral -1 mm to 1 mm) were studied. Maximum intensity of Z-stack projections were obtained and Sholl analysis was performed as previously described (Norris et al., 2014) using the Sholl Analysis tool in Fiji (Ferreira et al., 2014). 4–7 animals per treatment were used.

#### 2.3.3. Morphometric studies

Every sixth sagittal section of the cerebellum was stained with cresyl violet and observed using a microscope (Olympus CX31, Buenos Aires, Argentina) and an Infinity1 camera (Lumera Corporation, Ottawa, ON, Canada). All measurements were performed with the aid of Fiji software (Schindelin et al., 2012), drawing the perimeter of lobule 7 (L7) to obtain the area, a line at the apex of L7 to measure the thickness of the molecular layer, and the perimeter of Purkinje cells (PCs) to calculate the PC size. The linear density of PCs was determined as the number of neurons counted along a line drawn on the PC layer. Examples are shown in Supplementary Fig. 1. Measurements were performed in three sections per animal, and 3–5 animals per experimental group were used.

### 2.4. LPS challenge

Mice that had not been behaviorally tested were injected intraperitoneally with 25 μg/kg lipopolysaccharides (*Escherichia coli* LPS, serotype 0111:B4, Sigma-Aldrich, St. Louis, USA) or with sterile saline solution (SAL) between PD60 and PD67 (first and second cohort), or at PD21 (third cohort). Animals were challenged between 9:00 and 10:00 am, to avoid the effect of normal corticosterone circadian variations. Animals were deeply anesthetized and sacrificed two hours after LPS injection, when there is a peak in circulating corticosterone levels (Pitossi et al., 1997). Animal's trunk blood was collected from the heart in heparinized tubes.

### 2.5. Corticosterone radioimmunoassay (RIA)

Corticosterone plasma levels were measured by means of RIA as previously described (Kazlauskas et al., 2016; Lucchina et al., 2010). The assay was performed following the RIA protocol provided by the anti-corticosterone antibody manufacturer (C8784, Sigma-Aldrich, St. Louis, USA) using $^{3}$H-corticosterone (1,2,6,7-$^{3}$H(N)-corticosterone, Perkin-Elmer, Waltham, MA, USA).

### 2.6. Real time PCR

Animals from the fourth cohort were sacrificed by cervical dislocation between PD60 and PD67, and cerebellar tissue was rapidly removed and frozen in liquid nitrogen. RNA purification and reverse transcription were performed as previously described (Depino et al., 2005). Real-time PCR was carried out on cDNA using the SYBR-green I fluorescence method (Lucchina and Depino, 2014), in a StepOnePlus Real-Time PCR System (Thermo Fisher Scientific). Standard curves were run along with the samples, and calculated cDNA dilution values were normalized with cDNA levels of β-actin in the same samples. We used the following primers: Arg-1, forward 5′-GTGAAGAACCCACGGT CTGT, reverse 5′- GCCAGAGATGCTTCCAACTG; IL-1β, forward 5′-ACAGAATATCAACCAACAAGTGATATTCTC, reverse 5′- GATTCYYYC-CTTTGAGGCCCA; β-actin, forward 5′- CCACACCCGCCACCAGTTC, reverse, 5′- GACCCATTCCCACCATCACACC. All samples were run in triplicates. Specificity was controlled by melting curves and electrophoresis on agarose gels.

### 2.7. Statistical analysis

Sample sizes were estimated based on similar, previously conducted studies. No statistical methods were used to determine sample size. Data graphs were created using GraphPad Prism (Version 5; GraphPad Software Inc., La Jolla, CA) and results are presented as mean + SEM. For the social interaction test, where animals from the same litter were evaluated, a nested two-way analysis of variance (ANOVA) was used with litter as a subgroup, using InfoStat software (Version 2016, InfoStat Group, Córdoba National University, Córdoba, Argentina). To compare the time spent in each of the arena's compartment, a paired Student's *t*-test was used. For the RIA, glial cell, morphometric and RT-PCR analyses, only one animal per litter was used; hence, two or three-way ANOVA of normally distributed data was performed using the Statistica software (Version 8, StatSoft Inc., Tulsa, OK, USA). Whenever appropriate, Fisher's LSD posthoc test was used as not all pairwise comparisons were made. Normality was confirmed by the D'Agostino & Pearson omnibus normality test. The statistical designs and outcomes are outlined in Supplementary tables 1-6. In all cases, statistical significance was assumed where $p < 0.05$.

## 3. Results

### 3.1. Prenatal VPA administration reduces sociability levels only in male mice

One of the main behavioral alterations of ASD is the social interaction deficit. It was previously shown that prenatal exposure to VPA results in reduced sociability in male mice [e.g. (Campolongo et al., 2018)]. Here, we analyzed male and female littermates, to compare both the effects of sex and VPA prenatal treatment on social interaction levels in mice (Fig. 1A). Animals were exposed to a novel, young, sex-matched animal in the social interaction test, and we quantified the time the test mouse spent sniffing the social stimulus or the novel object (Fig. 1B). Female mice showed a preference for exploring the social stimulus over the novel object, regardless of the prenatal treatment (Paired Student's t test, female Veh: $t_{(12)} = 2.633$, $p = 0.022$; female VPA: $t_{(10)} = 2.577$, $p = 0.028$). Male control mice also showed this preference ($t_{(14)} = 3.801$, $p = 0.002$), but males prenatally exposed to VPA spent a similar amount of time exploring the social and the non social novelties ($t_{(17)} = 1.558$; $p = 0.138$). To specifically test the effect of sex on sociability and its interaction with the prenatal treatment, we calculated the percentage of time that each animal spent exploring the social stimulus (Fig. 1C). A nested two-way ANOVA showed a prenatal treatment effect ($F_{(1, 40)} = 6.37$, $p = 0.025$) and a sex effect ($F_{(1, 40)} = 4.13$, $p = 0.045$). While male VPA mice showed reduced sociability levels, female VPA mice explored the social stimulus similarly to female Veh mice. These results show that prenatal VPA administration affects social interaction levels in a sex-specific manner in adult animals.

### 3.2. Prenatal VPA exposure affects peripheral inflammatory response in male but not in female offspring

LPS injection has been widely used to mimic a bacterial infection, triggering an acute inflammatory response. To evaluate the peripheral

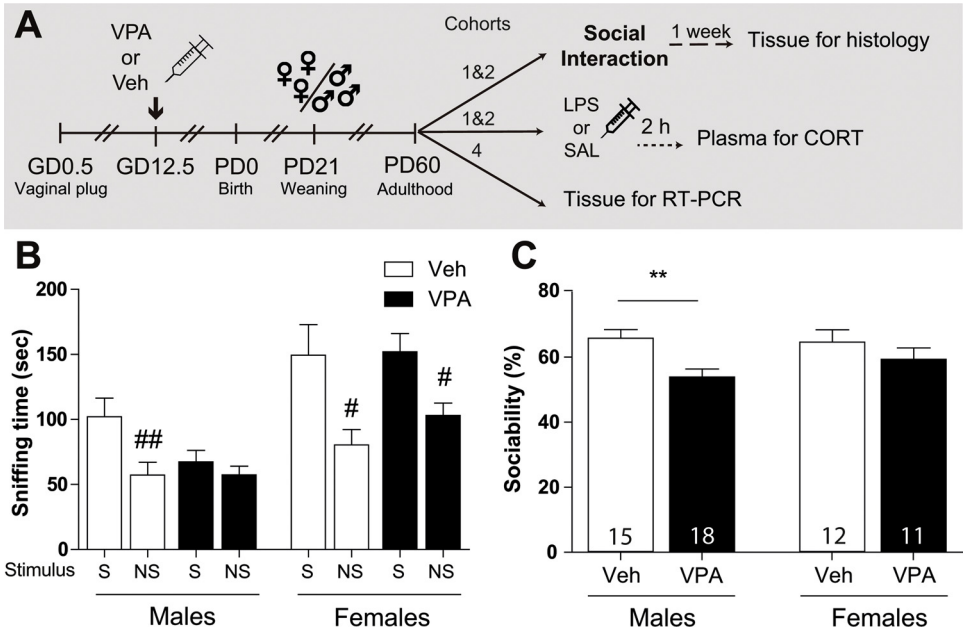


**Fig. 1.** Prenatal exposure to VPA leads to reduced social interaction only in male mice. (A) A timeline for the generation of VPA and control mice, their behavioral testing and plasma and tissue preparation. (B) Time spent sniffing the stimulus mouse (S) or the novel object (NS) in a three-chamber social interaction test for control (Veh) and VPA-exposed animals. Male VPA mice do not show the typical social preference observed in all other groups. (C) VPA-exposed males show a reduction in the percentage of time spent sniffing the stimulus mice. *Ns* are specified within the bars in (C). Paired Student's t test: # $p <$ 0.05, ## $p < 0.01$. Fisher's LSD Test: ** $p <$ 0.01. Mean + SEM. S, social side; NS, non social side.

immune response in male and female offspring, we measured corticosterone (CORT) levels 2 h after a LPS or saline (SAL) intraperitoneal injection (Fig. 1A). CORT is the main hormonal output of the hypothalamus-pituitary-adrenal (HPA) axis, which is activated by peripheral LPS challenge (Lucchina and Depino, 2014) and affected in various psychiatric disorders and animal models with altered sociability (Sandi and Haller, 2015).

LPS injection activated the HPA axis in all animals, causing higher CORT release, as expected (Fig. 2). However, a three-way ANOVA revealed a sex effect ($F_{(1,\ 34)} = 10.14$, $p =$ 0.003), an inflammatory challenge effect ($F_{(1,\ 34)} = 120.01$, $p <$ 0.001) and an interaction between sex, prenatal treatment and inflammatory challenge ($F_{(1,\ 34)} = 7.14$, $p =$ 0.012). In particular, CORT basal levels were altered by VPA exposure in a sex-specific way: Male VPA-SAL mice showed higher CORT levels than Veh-SAL males, and also than VPA-SAL females. Conversely, basal CORT release was similar in VPA and Veh females (Fig. 2).

These results show that basal CORT levels are increased only in VPA male offspring, whilst all animals show a normal HPA axis response to this inflammatory challenge.

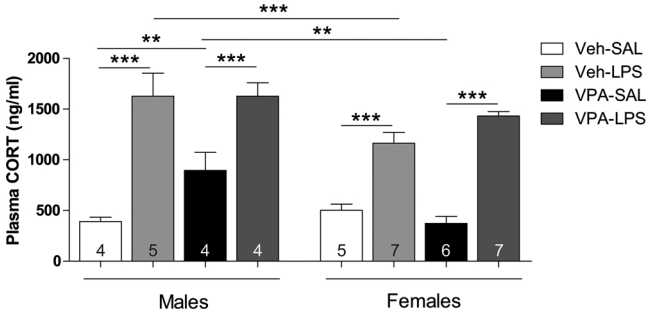


**Fig. 2.** Male VPA mice show increased basal corticosterone levels in adulthood, but a normal response to an inflammatory stimulus. All animals show a typical increase in corticosterone (CORT) plasma levels 2 h after the administration of an inflammatory stimulus (LPS). VPA-exposed males show increased CORT levels when injected with saline (SAL). *Ns* are specified within the bars. Fisher's LSD Test: ** $p <$ 0.01, *** $p <$ 0.001. Mean + SEM.

### 3.3. VPA administration affects the neuroinflammatory state in adult animals in a sex-specific manner

With the aim to characterize the central inflammatory state, we studied astroglial and microglial activation in adult offspring of VPA- and Veh-injected dams. We quantified the cell density of astrocytes and the GFAP-positive area, and the cell density of each microglial cell type to estimate activation levels. We focused our analysis on the cerebellum, as we have previously observed alterations in glial cells in this area (Kazlauskas et al., 2016; Lucchina and Depino, 2014), and it can modulate social behavior (Lucchina and Depino, 2014). In addition, we evaluated glial cells in the hippocampus to assess the specificity of the alterations observed, comparing the cerebellum with another region involved in social behavior (Depino et al., 2011), which also shows glial cells alterations during postnatal development after VPA exposure (Kazlauskas et al., 2016).

#### 3.3.1. Cerebellum

We have previously shown that eliciting inflammation in the lobule 7 of the cerebellum results in reduced sociability in the mouse (Lucchina and Depino, 2014). To evaluate if prenatal VPA can affect differently female and male cerebella, we studied astroglial and microglial activation in the adult lobule 7 of both sexes. We subdivided this region into the molecular and granular cell layers and counted the number of microglial cells. As the morphology of the cerebellar astrocytes prevented us from distinguishing one cell from another, we measured the GFAP-positive area.

For astrocytes (Fig. 3A-D), a two-way ANOVA revealed a VPA effect on the molecular layer ($F_{(1,\ 14)} = 4.63$, $p =$ 0.049): female VPA mice show a bigger GFAP-positive area than Veh females (Fig. 3A). Also, we found a sex effect on the granular cell layer ($F_{(1,\ 14)} = 10.38$, $p =$ 0.006), as VPA females show an increased GFAP-positive area when compared to male VPA mice (Fig. 3B).

Results were very similar for microglia (Fig. 3E-O). We found a prenatal treatment effect in the molecular layer for total and ramified microglial cells ($F_{(1,\ 14)} = 4.74$, $p =$ 0.047; and $F_{(1,\ 14)} = 5.78$, $p =$ 0.031, respectively), where VPA animals showed increased cell density levels (Fig. 3E). However, the density of hypertrophic microglial cells was unaltered by prenatal treatment and similar in both sexes (Fig. 3E, right panel). We found a tendency in the interaction between prenatal treatment, sex and diameter for the number of branches in Sholl

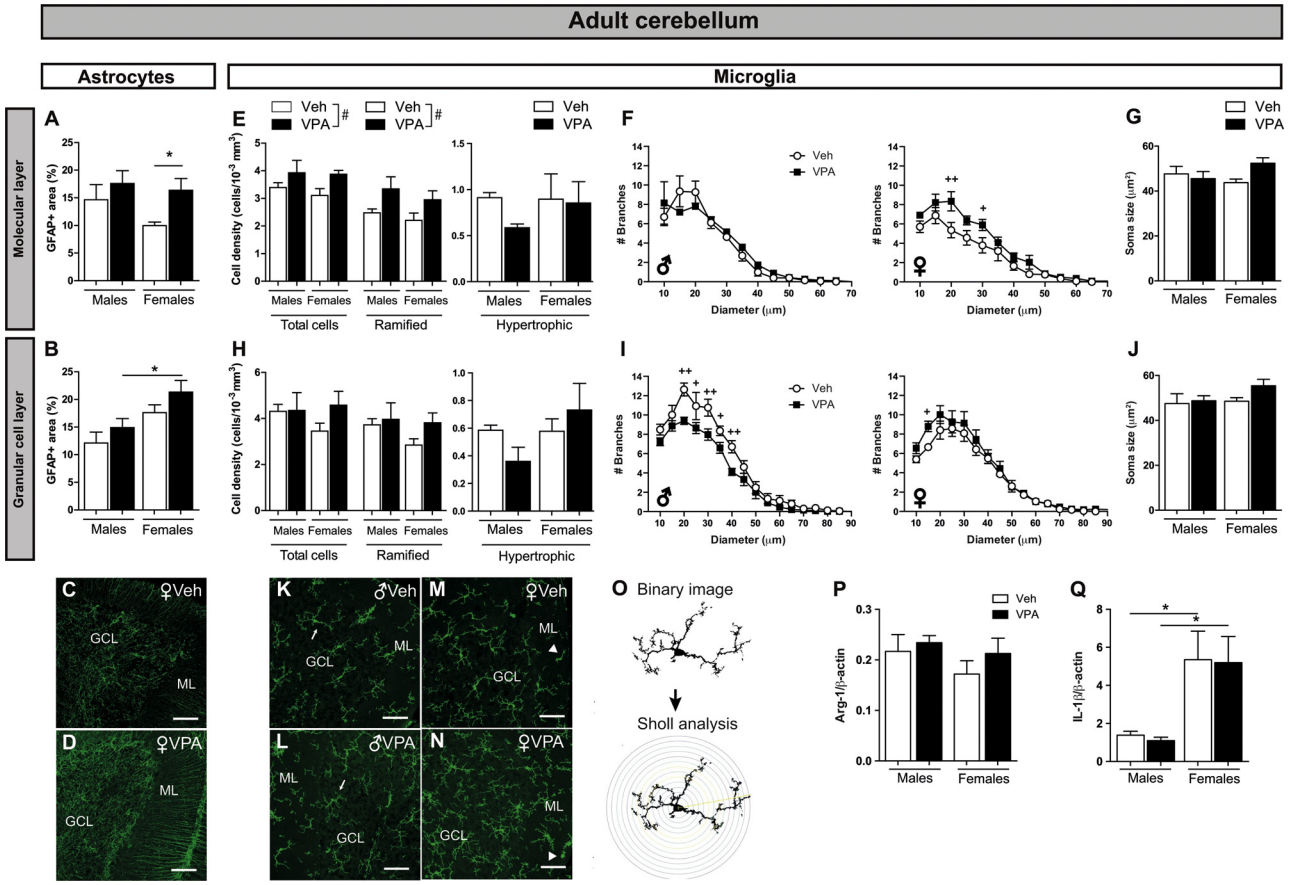


**Fig. 3.** VPA effects on glial activation in the lobule 7 of the cerebellum are more pronounced in adult female mice. GFAP-positive area was quantified in the molecular layer (A) and granular cell layer (B) of the lobule 7 of the cerebellum. Representative confocal microscopy photographs of anti-GFAP immunofluorescence performed on female Veh (C) and VPA (D) mice. Analysis of microglia was performed in the molecular (E–G) and granular cell layer (H–J). Total cell number (E and H) is mainly composed of ramified cells (left panels), while few hypertrophic cells are observed (right panels). Sholl analysis (F and I) and soma size measurements (G and J) are shown. Representative confocal microscopy photographs of anti-Iba1 immunofluorescence performed on male Veh (K) and VPA (L) and female Veh (M) and VPA (N) mice. Arrows show examples of ramified microglia, and arrowheads of hypertrophic cells. Scale bar, 50 μm. GCL, granular cell layer; ML, molecular layer. Sholl analysis for the microglia marked with an arrow in K is performed by creating the binary image to calculate the number of branches (O). $N = 4$–5 mice per group. Arginase-1 (P) and interleukin-1β (Q) expression were quantified by RT-PCR. $N = 5$–7 mice per group. Prenatal treatment effect in ANOVA: # $p < 0.05$. Fisher's LSD Test: * $p < 0.05$. Pairwise comparisons between Veh and VPA: + $p < 0.05$, + + $p < 0.01$. Mean + SEM.

analysis ($F_{(12,\ 168)} = 1.80$, $p = 0.052$), due to an increase in the number of branches in VPA-exposed females (Fig. 3F, right). No differences were observed in the size of the soma, although a tendency was observed for an interaction between prenatal treatment and sex ($F_{(1,\ 14)} = 1.80$, $p = 0.052$) (Fig. 3G).

No alterations were observed for microglial cells in the granular cell layer (Fig. 3H), although the same tendency of increased numbers of total cells in VPA-exposed animals can be observed. Interestingly, an interaction between prenatal treatment, sex and diameter was observed after Sholl analysis ($F_{(16,\ 224)} = 2.43$, $p = 0.0021$; Fig. 3I), with microglia of VPA-exposed males having less ramifications than control males and VPA-exposed females more ramifications than Veh females. These differences were observed in the smaller diameters, suggesting a more hypertrophic phenotype in Veh males and VPA females. No differences were observed in the size of microglia soma in this layer (Fig. 3J).

Finally, no differences were observed in the levels of Arginase-1 mRNAs (Fig. 3P), but female mice expressed more IL-1β in the cerebellum, when compared with males, regardless of prenatal treatment ($F_{(1,\ 18)} = 12.73$, $p = 0.002$; Fig. 3Q).

These results show that male and female animals prenatally exposed to VPA have altered astroglia and microglia in the adult cerebellum. Even more, this effect appears to be higher in female animals in some regions, such as the astrocytic activation in the granular cell layer. However, some sex-related differences are unaltered by prenatal VPA exposure, as can be observed for IL-1β mRNA levels in the cerebellum.

### 3.3.2. Hippocampus

Within the hippocampus, we analyzed the dentate gyrus (DG) and CA1 region and estimated the GFAP-positive cell density and microglial cell density. Only ramified cells are reported because we did not observe hypertrophic or ameboid/round cells in the majority of the animals studied. Results are presented in Fig. 4.

The DG was subdivided into three areas: molecular layer, granular cell layer, and hilus. In the astroglial analysis, we found a prenatal treatment effect in the granular cell layer ($F_{(1,\ 15)} = 5.48$, $p = 0.034$), where female VPA mice exhibit increased astrocyte cell density (Fig. 4C). Similar results were found for microglia, as the statistical analysis revealed a prenatal treatment effect in the molecular layer ($F_{(1,\ 19)} = 10.16$, $p = 0.005$), where VPA females present increased density of microglial cells (Fig. 4B). A sex effect was found in the hilus, both for astroglial ($F_{(1,\ 15)} = 22.83$, $p < 0.001$) and microglial ($F_{(1,\ 19)} = 28.84$, $p < 0.001$) cell density analyses. Interestingly, females present higher astrocyte density than males (Fig. 4E), but decreased microglial cell density (Fig. 4F).

CA1 was also subdivided into three areas: *stratum oriens*, pyramidal cell layer and *stratum radiatum*. We found no differences in astroglial or microglial cell density in the *stratum oriens* (Figs. 4G-H) or *stratum*

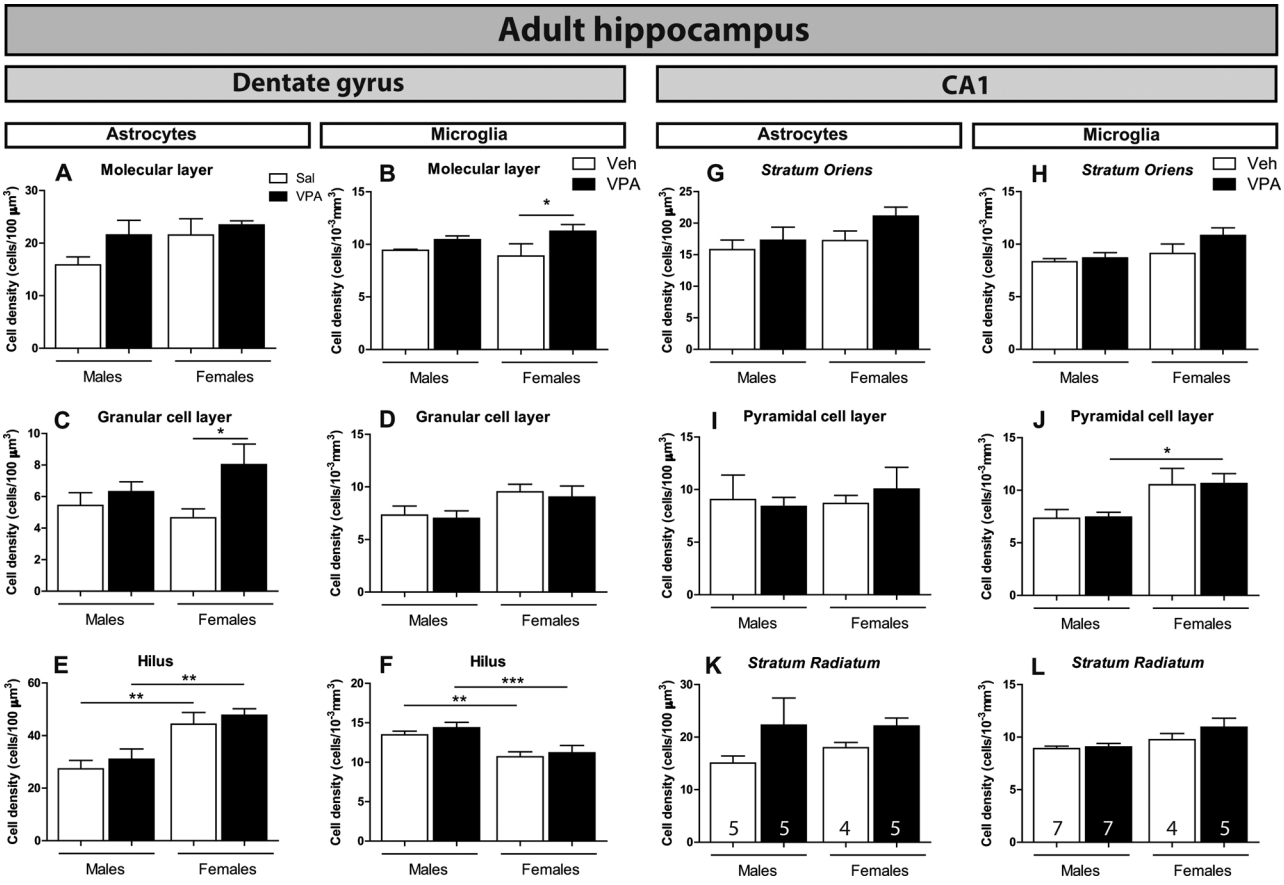


**Fig. 4.** Prenatal VPA exposure affects glial activation in the female dentate gyrus of the hippocampus. Astrocyte and microglia cell densities were quantified in the molecular layer (A and B), granular cell layer (C and D) and hilus (E and F) of the dentate gyrus, and in the *stratum oriens* (G and H), pyramidal cell layer (I and J) and *stratum radiatum* (K and L) of CA1. *Ns* are specified within the bars in (K) and (L). Fisher's LSD Test: * $p < 0.05$, ** $p < 0.01$, *** $p < 0.001$. Mean + SEM.

*radiatum* (Fig. 4K-L), but a sex effect on microglial cell density in the pyramidal cell layer ($F_{(1,\ 19)} = 8.62$, $p = 0.009$), where female VPA mice show higher cell density than males (Fig. 4J).

These results show that prenatal VPA treatment generates an increase both in astroglial and microglial cell density levels in the DG, which appear to be more pronounced in female mice. These results go in the same line of those observed in the cerebellum.

### 3.4. The peripheral inflammatory response and cerebellar glial cells show sex differences at PD21

So far, we have shown that VPA administration affects sociability, peripheral inflammatory response and the neuroinflammatory state in a sex-specific manner in adult animals. We aimed to explore if these sex differences were present in early stages of development, or alternatively, they aroused in adulthood. In a previous study (Kazlauskas et al., 2016), we found evidence that neuroinflammatory signs emerge during the postnatal period in female VPA mice and become evident at PD21. Moreover, at PD21 male offspring prenatally exposed to VPA shows altered sociability (Campolongo et al., 2018). So, we evaluated the peripheral inflammatory response and neuroinflammatory state in both male and female mice at PD21 (Fig. 5A).

#### 3.4.1. Peripheral inflammatory response

At PD21, basal CORT levels were similar in male and female mice, and the statistical analysis revealed an inflammatory challenge effect ($F_{(1,\ 32)} = 37.23$, $p < 0.001$) due to increased CORT release after LPS injection in all animals (Fig. 5B). Although both Veh and VPA female mice showed a significant HPA axis activation, the LPS-induced CORT release in PD21 males did not reach significance, showing a hypoactivation of the HPA axis when compared to females. Indeed, we found a sex effect ($F_{(1,\ 32)} = 10.24$, $p = 0.003$) and an interaction between sex and inflammatory challenge ($F_{(1,\ 32)} = 6.43$, $p = 0.016$), due to a higher inflammatory response both in Veh and VPA females than in males (Fig. 5B).

These results show sex differences in the response to inflammatory stimuli in young animals. However, this disparity is not affected by prenatal exposure to VPA. When compared with adult animals, we observed a different pattern of CORT levels: the female higher response at PD21 is followed by a lower response in adult females. In addition, the higher basal CORT levels observed in adult males is not observed in younger (PD21) animals.

#### 3.4.2. Astroglia and microglia

*3.4.2.1. Cerebellum.* A two-way ANOVA showed a strong statistical tendency for a VPA effect on GFAP-positive area in the molecular layer of the lobule 7 ($F_{(1,\ 15)} = 4.28$, $p = 0.056$) and a significant interaction between sex and prenatal treatment ($F_{(1,\ 15)} = 7.67$, $p = 0.014$). Control females showed an increased astrocyte area, while VPA reversed this sex effect (Fig. 5C). The results were similar for the granular cell layer, where we also found a significant interaction between sex and prenatal treatment ($F_{(1,\ 15)} = 11.36$, $p = 0.004$) and a decreased GFAP-positive area in VPA females (Fig. 5D).

Microglial cell density levels were altered in the molecular layer of the cerebellum, as a VPA effect was found for total and ramified microglial cells ($F_{(1,\ 15)} = 6.74$, $p = 0.020$, and $F_{(1,\ 15)} = 5.27$, $p = 0.037$, respectively). VPA animals showed higher microglial cell density levels than Veh mice, but only VPA females showed a significant increase in ramified cell density levels (Fig. 5E). A sex effect was found for hypertrophic cell density in the molecular layer ($F_{(1,\ 15)} = 15.83$, $p =$

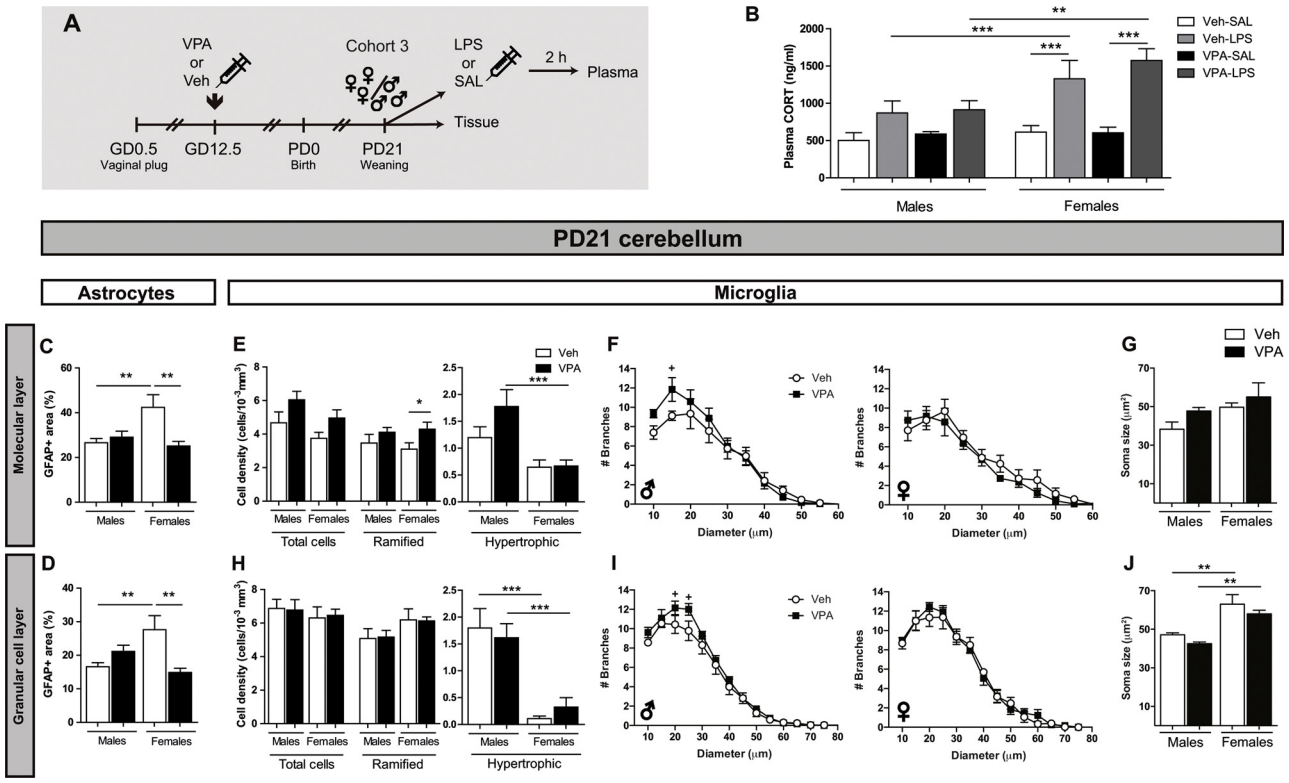


**Fig. 5.** Females show a higher peripheral inflammatory response than males at PD21, and a differential glial response to VPA. (A) Experimental timeline for the analyses of young animals. (B) All animals show a typical increase in corticosterone (CORT) plasma levels 2 h after the administration of an inflammatory stimulus (LPS), but this increase is higher in females than males. N = 5 mice per group. GFAP-positive area was quantified in the molecular layer (C) and granular cell layer (D) of the lobule 7 of the cerebellum, where control females show the highest values. Analysis of microglia was performed in the molecular (E–G) and granular cell layer (H–J). VPA animals show an increase in microglial cell density in the molecular layer (E, left) but not in the granular cell layer (H, left). More hypertrophic cells are observed in males (E and H, right panels). Sholl analysis shows increased ramification of VPA male microglia (F and I). Microglia soma size is larger for female animals in the granular cell layer (J), but not the molecular layer (G). $N = 4$–5 mice per group. Fisher's LSD Test: $^{*}p < 0.05$, $^{**}p < 0.01$, $^{***}p < 0.001$. Pairwise comparisons between Veh and VPA: $+\ p < 0.05$, $++\ p < 0.01$. Mean + SEM.

0.001), where males presented more of these cells (Fig. 5E, right). VPA-exposed males also presented microglial cells with more branches in the inner circles of Sholl analysis, suggesting a more hypertrophic phenotype in this area (Fig. 5F, left). We found no effect of VPA or sex on the size of microglia soma in the cerebellum of PD21 mice (Fig. 5G).

We observed no alterations in total and ramified microglial cell density levels in the granular cell layer (Fig. 5H, left). However, a sex effect was found for hypertrophic cells ($F_{(1,\ 15)} = 43.39$, $p < 0.001$), where males presented more of these cells than females (Figs. 5H, right). In this region microglial cells also showed more branches in the VPA males (Fig. 5I, left). The size of the microglia soma was smaller in males than in females ($F_{(1,\ 15)} = 29.23$, $p < 0.001$; Fig. 5J).

As in the case of adult male mice, at PD21 male VPA mice did not show remarkable alterations in glial activation in the lobule 7 of the cerebellum. On the contrary, female VPA mice showed increased ramified microglial cell density in the molecular layer and decreased GFAP-positive area both in the molecular and granular cell layers of the cerebellum. These results show that glial alterations in the cerebellum in female VPA animals appear at early developmental stages. Remarkably, the reduced GFAP-positive area observed in PD21 VPA female mice is followed by an increase in these animals in adulthood, suggesting a compensatory effect.

*3.4.2.2. Hippocampus.* Two-way ANOVAs showed a sex effect on the density of GFAP-positive cells in all regions (DG-Molecular layer: $F_{(1,\ 15)} = 4.511$, $p = 0.051$; DG-Granular cell layer: $F_{(1,\ 15)} = 65.616$, $p < 0.001$; DG-*Hilus*: $F_{(1,\ 15)} = 10.119$, $p = 0.006$; CA1-*Stratum oriens*: $F_{(1,\ 15)} = 8.570$, $p = 0.010$; CA1-Pyramidal cell layer: $F_{(1,\ 15)} = 19.016$, $p < 0.001$; CA1-*Stratum radiatum*: $F_{(1,\ 15)} = 12.752$, $p = 0.003$), with female mice having more astroglial cells than males (Supplementary Fig. 2).

Conversely, microglial cell density showed a sex effect in the DG-Granular cell layer ($F_{(1,\ 16)} = 13.706$, $p = 0.002$), the CA1-*Stratum oriens* ($F_{(1,\ 16)} = 8.787$, $p = 0.009$) and the CA1-*Stratum radiatum* ($F_{(1,\ 16)} = 13.015$, $p = 0.002$), with female mice having less microglial cells than males (Supplementary Fig. 2D, H and L). In addition, we observed a prenatal treatment effect in the DG-Molecular layer ($F_{(1,\ 16)} = 5.997$, $p = 0.026$) and the DG-*Hilus* ($F_{(1,\ 16)} = 12.437$, $p = 0.003$), with VPA-exposed animals having more microglial cells than control offspring (Supplementary Fig. 2B and F).

These results show that female mice present more astrocytes in the hippocampus at PD21 than male littermates and suggest that microglial cells in the dentate gyrus are affected by prenatal exposure to VPA in both sexes at this age. In the hippocampus, a similar pattern of VPA effects are observed in young and adult animals.

### 3.5. Absence of neuronal alterations in the cerebellum of adult VPA-exposed mice

A previous study has shown that animals exposed to maternal immune activation (MIA) have less Purkinje cells (PCs) in the lobule 7 (L7) of the cerebellum (Shi et al., 2009). MIA also leads to reduced sociability (Malkova et al., 2012). We evaluated the effect of VPA exposure on cerebellar neurons.

We found no effect of prenatal VPA exposure on the area of L7 (Fig. 6A) or the size of PCs (Fig. 6C). However, we found an interaction between prenatal treatment and sex on the thickness of the molecular layer (ML) at the apex of L7 ($F_{(1,\ 15)} = 4.73$, $p = 0.046$), with female

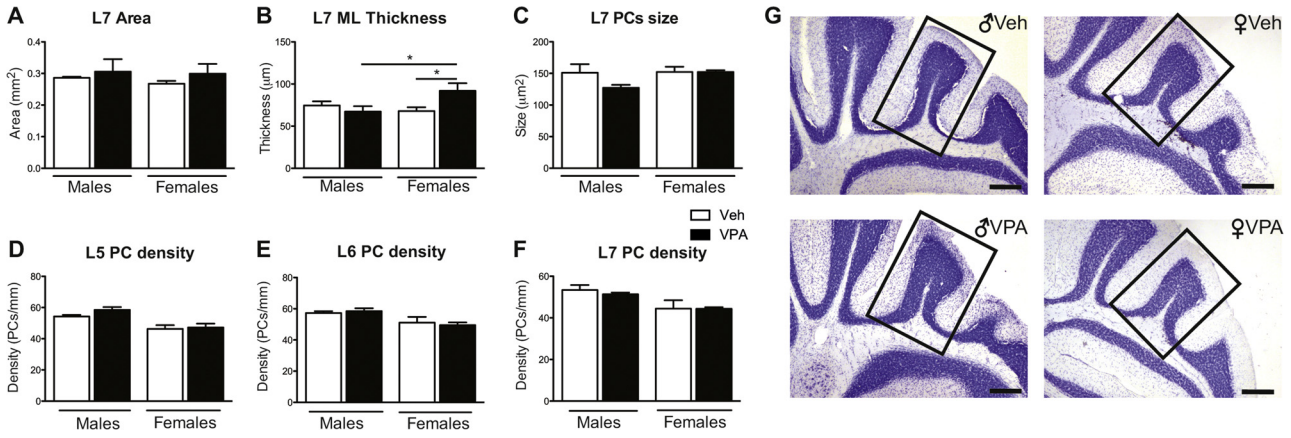


**Fig. 6.** Female VPA mice show increased thickness of the molecular layer of the lobule 7 in the adult cerebellum, but normal Purkinje cell density. (A) Area of lobule 7 (L7) is similar in all animals. (B) Thickness of the molecular layer (ML) of the L7 is increased in female VPA mice. (C) Size of the Purkinje cells (PCs) of L7 is unaltered by VPA treatment. Density of PCs in the lobule 5 (D), 6 (E) and 7 (F) is not affected by VPA treatment, but it is higher in male mice. (G) Representative images of Nissl-stained cerebella, where the L7 is outlined. Scale bar, 0.2 mm. $N$ = 4–5 mice per group. Fisher's LSD Test: * $p < 0.05$. Mean + SEM.

mice prenatally exposed to VPA having a thicker ML than male littermates or control females (Fig. 6B). Finally, we found no effect of prenatal treatment on PCs density, but female mice have less PCs than male littermates (sex effect, in L5: $F_{(1, 13)} = 20.94$, $p = 0.0005$; in L6: $F_{(1, 13)} = 13.58$, $p = 0.0027$; and L7: $F_{(1, 13)} = 17.27$, $p = 0.0011$; Fig. 6D-F). Representative photomicrographs of Nissl-stained cerebella where L7 is outlined are shown in Fig. 6G.

These results suggest that the glial alterations observed in the L7 of the cerebellum do not affect PCs. The increase in ML thickness in VPA female mice could, however, result from the increase in glial cells observed in these animals. The ML contains the dendritic trees of the PCs, the axons of granule cells, and the inhibitory interneurons, so glia could affect cerebellar function by affecting any of these cells.

## 4. Discussion

The results presented here show that female and male mice are differently affected by prenatal exposure to VPA, showing an interaction between this prenatal environmental factor and sex. Specific effects are observed in very distinct parameters such as social behavior, peripheral inflammatory response and central neuroimmunological cells. In addition, we show that glial cells are sexually dimorphic, displaying different densities and morphologies in male and female mice.

Although several effects of prenatal VPA exposure on female offspring have been reported (Hara et al., 2012; Kim et al., 2013; Mowery et al., 2015; Perez-Pouchoulen et al., 2016; Schneider et al., 2008), most of the studies using VPA-exposed animals have focused on males. To our knowledge, this is the first time that a characterization of the central and peripheral inflammatory status, and their comparison with alterations in sociability, has been performed, emphasizing the study of female subjects and contrasting them with their male siblings.

We observed an interaction between prenatal VPA exposure and sex in sociability levels. In particular, male VPA mice showed decreased sociability levels in the social interaction test, while VPA females showed normal social exploration levels. These results agree with other reports, in which reduced sociability has been observed in young and adult VPA male rats but not in VPA females (Kim et al., 2013; Schneider et al., 2008). This characteristic of the VPA model gives it strong value to study mechanisms of resilience and susceptibility in biological processes that modulate sociability, a behavioral domain affected in many different psychiatric disorders in addition to ASD, including schizophrenia, anxiety and depression. Worth to mention, however, the prevalence of ASD in children prenatally exposed to VPA is even in girls and boys (Rasalam et al., 2005). A possible explanation for this discrepancy could be the specific effects that can be achieved by a sole injection of VPA at a critical age in development (GD12.5), an age when another disrupting, environmental stimulus, i.e. maternal immune activation, can also result in altered sociability in a sex-dependent manner (Haida et al., 2019).

In addition, males prenatally exposed to VPA show elevated plasma concentration of CORT when adults. Previous work has shown that female rodents release more CORT than males both basally (Critchlow et al., 1963) and upon restraint stress (Figueiredo et al., 2002). Hence, increased CORT levels in VPA males is unusual and may have multiple effects on the animals. CORT can affect brain development and the consolidation of circuits relevant to behavior (McEwen, 2008). In particular, CORT could modulate the expression of CRH in the hippocampus, which has been correlated to changes in social recognition (Schaafsma et al., 2017). Interestingly, our results show that the increased CORT levels in males requires maturation over adolescence, as male mice display a blunted HPA response to LPS at PD21, with no alterations in the basal levels of CORT. How this alteration in CORT levels is elicited by prenatal exposure to VPA and established during adolescence to be evident in adult males, needs to be further explored.

The neuroinflammatory state was also differently affected by VPA in males than in females. Interestingly, adult VPA females show a general tendency to have more glial cells, both in the cerebellum and in the hippocampus. Moreover, the increase in the number of branches of cerebellar microglial cells suggests a more hypertrophic morphology in VPA females. However, the temporal establishment of these differences appears to be specific to each area. For example, in the cerebellum, VPA females show less GFAP-positive area at PD21 and more as adults, suggesting a compensatory effect. In addition, adult females prenatally exposed to VPA have increased astrocyte cell density in the granular cell layer and more microglial cells in the molecular layer of the DG. These VPA effects are less evident at weaning, probably because at PD21 sex differences are more salient and they may prevent us from detecting significant effects of prenatal treatment in this experimental design. Indeed, in a previous study we were able to detect a significant effect of VPA on hippocampal glial cells during postnatal development by only studying female offspring (Kazlauskas et al., 2016). The continuous presence of abnormal numbers of glial cells in the hippocampus could be a consequence of VPA effects on either glial cells or neurons.

In contrast, the cerebellum and hippocampus of VPA male mice did not show clear signs of glial activation at weaning or in adulthood. This phenomenon could be due to differences in the glial response, as there is a large amount of evidence of sex differences in glial morphology and its correlation with neuronal morphology. We chose the postnatal age PD21 based on our previous report showing more differences in female VPA animals at that age (Kazlauskas et al., 2016). However, we may

have missed earlier differences in VPA males that could affect normal development (Perez-Pouchoulen et al., 2015). Indeed, a critical period for inflammation altering cerebellar development and social play in males has been identified during the second postnatal week (Hoffman et al., 2016).

Based on these results, we believe that prenatal VPA administration causes sex-specific effects on social behavior and the inflammatory response because it is acting upon different brain substrates. Naturally present sexual dimorphisms could be generating different reactions after the same stimulus during development, eliciting divergent long-term consequences. For example, the normal development of microglial progenitors could be altered by the early epigenetic effects of VPA. The hyperacetylation wave after VPA administration at GD12.5 (Kataoka et al., 2013) could generate a disruption in microglial migration and CNS colonization, affecting also its morphology and function. Indeed, there is a sexual dimorphism in the microglial colonization, morphological alterations and phagocytic action in the brain during development (Perez-Pouchoulen et al., 2015; Schwarz and Bilbo, 2012). Given the essential role that microglial cells fulfill during brain development, this could affect its normal development and alter sociability (Paolicelli et al., 2011; Zhan et al., 2014).

In adult animals, these differences could be exacerbated by the action of sexual hormones, given that in general terms estrogens promote glial activation while testosterone inhibits it (Barreto et al., 2007; Habib and Beyer, 2015; Sierra et al., 2008). Indeed, females express higher levels of IL-1β in the cerebellum than males, suggesting a general proinflammatory sex-related bias. Moreover, we have observed glial activation in female VPA mice, and not in males, throughout the postnatal period and even in adulthood.

In summary, VPA administration produces sex-specific effects on glial activation at PD21 and adulthood, and on basal CORT levels and social behavior in adult animals. Along with our previous study of the early postnatal period in females (Kazlauskas et al., 2016), these results contribute to achieve an exhaustive characterization of inflammatory alterations both in male and female animals prenatally exposed to VPA. This complements previous studies conducted in male VPA mice (Schneider and Przewlocki, 2005; Schneider et al., 2006) and allows us to perform comparative analyses to facilitate the comprehension of the mechanisms behind VPA effects in both sexes.

Our results show that prenatal exposure to VPA have different long-term consequences on peripheral CORT response and neuroinflammation when male and female animals are compared. In brief, VPA induces a neuroinflammatory state that is more pronounced in females. However, only VPA males show the reduction in sociability. Thus, our results suggest that the neuroinflammatory state previously observed in people with ASD (Lee et al., 2017; Morgan et al., 2010; Vargas et al., 2005) should be taken cautiously, as it could either reflect a pathological pathway, as observed in VPA male mice, or a defensive response, as the one observed in VPA female mice. The precise linkage between neuroinflammation and sociability needs to be further studied.

We hope that these studies could help identify resilient mechanisms acting on females, which could explain the 4:1 incidence observed in ASD. Moreover, they could contribute to our understanding of the specific symptoms observed in girls with ASD. Finally, we cannot rule out that there are factors giving a higher susceptibility to boys, which could also be identified by this kind of studies.

## Declaration of Competing Interest

None.

## Acknowledgements

This work was supported by the National Agency of Promotion of Science and Technology (ANPCyT) (PICT2013-1362); and the University of Buenos Aires (UBACyT2016). A.M.D. is a member of the Research Career of the National Council of Scientific and Technological Research (CONICET), Argentina and Professor at the Faculty of Exact and Natural Sciences, University of Buenos Aires, Argentina. N.K., A.S., M.C. and C.Z. are fellows of the CONICET.

## Appendix A. Supplementary data

Supplementary material related to this article can be found, in the online version, at doi:https://doi.org/10.1016/j.psyneuen.2019.104441.

## References

American Psychiatric Association, 2013. Diagnostic and Statistical Manual of Mental Disorders, fifth ed. .

Barreto, G., Veiga, S., Azcoitia, I., Garcia-Segura, L.M., Garcia-Ovejero, D., 2007. Testosterone decreases reactive astroglia and reactive microglia after brain injury in male rats: role of its metabolites, oestradiol and dihydrotestosterone. Eur. J. Neurosci. 25, 3039–3046.

Campolongo, M., Kazlauskas, N., Falasco, G., Urrutia, L., Salgueiro, N., Hocht, C., Depino, A.M., 2018. Sociability deficits after prenatal exposure to valproic acid are rescued by early social enrichment. Mol. Autism 9, 36.

Centers for Disease Control and Prevention, 2009. Prevalence of Autism Spectrum disorders - Autism and Developmental Disabilities Monitoring Network, United States, 2006. Surveillance Summaries, MMWR.

Corbett, B.A., Mendoza, S., Abdullah, M., Wegelin, J.A., Levine, S., 2006. Cortisol circadian rhythms and response to stress in children with autism. Psychoneuroendocrinology 31, 59–68.

Critchlow, V., Liebelt, R.A., Bar-Sela, M., Mountcastle, W., Lipscomb, H.S., 1963. Sex difference in resting pituitary-adrenal function in the rat. Am. J. Physiol. 205, 807–815.

de Theije, C.G., Wopereis, H., Ramadan, M., van Eijndthoven, T., Lambert, J., Knol, J., Garssen, J., Kraneveld, A.D., Oozeer, R., 2014. Altered gut microbiota and activity in a murine model of autism spectrum disorders. Brain Behav. Immun. 37, 197–206.

Depino, A., Ferrari, C., Pott Godoy, M.C., Tarelli, R., Pitossi, F.J., 2005. Differential effects of interleukin-1beta on neurotoxicity, cytokine induction and glial reaction in specific brain regions. J. Neuroimmunol. 168, 96–110.

Depino, A.M., Lucchina, L., Pitossi, F., 2011. Early and adult hippocampal TGF-beta1 overexpression have opposite effects on behavior. Brain Behav. Immun. 25, 1582–1591.

Ferreira, T.A., Blackman, A.V., Oyrer, J., Jayabal, S., Chung, A.J., Watt, A.J., Sjostrom, P.J., van Meyel, D.J., 2014. Neuronal morphometry directly from bitmap images. Nat. Methods 11, 982–984.

Figueiredo, H.F., Dolgas, C.M., Herman, J.P., 2002. Stress activation of cortex and hippocampus is modulated by sex and stage of estrus. Endocrinology 143, 2534–2540.

Fombonne, E., 2003. Epidemiological surveys of autism and other pervasive developmental disorders: an update. J. Autism Dev. Disord. 33, 365–382.

Habib, P., Beyer, C., 2015. Regulation of brain microglia by female gonadal steroids. J. Steroid Biochem. Mol. Biol. 146, 3–14.

Haida, O., Al Sagheer, T., Balbous, A., Francheteau, M., Matas, E., Soria, F., Fernagut, P.O., Jaber, M., 2019. Sex-dependent behavioral deficits and neuropathology in a maternal immune activation model of autism. Transl. Psychiatry 9, 124.

Hara, Y., Maeda, Y., Kataoka, S., Ago, Y., Takuma, K., Matsuda, T., 2012. Effect of prenatal valproic acid exposure on cortical morphology in female mice. J. Pharmacol. Sci. 118, 543–546.

Hoffman, J.F., Wright, C.L., McCarthy, M.M., 2016. A critical period in purkinje cell development is mediated by local estradiol synthesis, disrupted by inflammation, and has enduring consequences only for males. J. Neurosci. 36, 10039–10049.

Kataoka, S., Takuma, K., Hara, Y., Maeda, Y., Ago, Y., Matsuda, T., 2013. Autism-like behaviours with transient histone hyperacetylation in mice treated prenatally with valproic acid. Int. J. Neuropsychopharmacol. 16, 91–103.

Kazlauskas, N., Campolongo, M., Lucchina, L., Zappala, C., Depino, A.M., 2016. Postnatal behavioral and inflammatory alterations in female pups prenatally exposed to valproic acid. Psychoneuroendocrinology 72, 11–21.

Kim, K.C., Kim, P., Go, H.S., Choi, C.S., Park, J.H., Kim, H.J., Jeon, S.J., Dela Pena, I.C., Han, S.H., Cheong, J.H., Ryu, J.H., Shin, C.Y., 2013. Male-specific alteration in excitatory post-synaptic development and social interaction in pre-natal valproic acid exposure model of autism spectrum disorder. J. Neurochem. 124, 832–843.

Kim, Y.S., Leventhal, B.L., Koh, Y.J., Fombonne, E., Laska, E., Lim, E.C., Cheon, K.A., Kim, S.J., Kim, Y.K., Lee, H., Song, D.H., Grinker, R.R., 2011. Prevalence of autism spectrum disorders in a total population sample. Am. J. Psychiatry 168, 904–912.

Lee, A.S., Azmitia, E.C., Whitaker-Azmitia, P.M., 2017. Developmental microglial priming in postmortem autism spectrum disorder temporal cortex. Brain Behav. Immun. 62, 193–202.

Lucchina, L., Carola, V., Pitossi, F., Depino, A.M., 2010. Evaluating the interaction between early postnatal inflammation and maternal care in the programming of adult anxiety and depression-related behaviors. Behav. Brain Res. 213, 56–65.

Lucchina, L., Depino, A.M., 2014. Altered peripheral and central inflammatory responses in a mouse model of autism. Autism Res. 7, 273–289.

Malkova, N.V., Yu, C.Z., Hsiao, E.Y., Moore, M.J., Patterson, P.H., 2012. Maternal immune activation yields offspring displaying mouse versions of the three core symptoms of autism. Brain Behav. Immun. 26, 607–616.

McEwen, B.S., 2008. Central effects of stress hormones in health and disease: understanding the protective and damaging effects of stress and stress mediators. Eur. J. Pharmacol. 583, 174–185.
Morgan, J.T., Chana, G., Pardo, C.A., Achim, C., Semendeferi, K., Buckwalter, J., Courchesne, E., Everall, I.P., 2010. Microglial activation and increased microglial density observed in the dorsolateral prefrontal cortex in autism. Biol. Psychiatry 68, 368–376.
Mowery, T.M., Wilson, S.M., Kostylev, P.V., Dina, B., Buchholz, J.B., Prieto, A.L., Garraghty, P.E., 2015. Embryological exposure to valproic acid disrupts morphology of the deep cerebellar nuclei in a sexually dimorphic way. Int. J. Dev. Neurosci. 40, 15–23.
Norris, G., Derecki, N., Kipnis, J., 2014. Microglial Sholl Analysis. Protocol Exchange.
Paolicelli, R.C., Bolasco, G., Pagani, F., Maggi, L., Scianni, M., Panzanelli, P., Giustetto, M., Ferreira, T.A., Guiducci, E., Dumas, L., Ragozzino, D., Gross, C.T., 2011. Synaptic pruning by microglia is necessary for normal brain development. Science 333, 1456–1458.
Perez-Pouchoulen, M., Miquel, M., Saft, P., Brug, B., Toledo, R., Hernandez, M.E., Manzo, J., 2016. Prenatal exposure to sodium valproate alters androgen receptor expression in the developing cerebellum in a region and age specific manner in male and female rats. Int. J. Dev. Neurosci. 53, 46–52.
Perez-Pouchoulen, M., VanRyzin, J.W., McCarthy, M.M., 2015. Morphological and phagocytic profile of microglia in the developing rat cerebellum. eNeuro 2.
Pitossi, F., del Rey, A., Kabiersch, A., Besedovsky, H., 1997. Induction of cytokine transcripts in the central nervous system and pituitary following peripheral administration of endotoxin to mice. J. Neurosci. Res. 48, 287–298.
Rasalam, A.D., Hailey, H., Williams, J.H., Moore, S.J., Turnpenny, P.D., Lloyd, D.J., Dean, J.C., 2005. Characteristics of fetal anticonvulsant syndrome associated autistic disorder. Dev. Med. Child Neurol. 47, 551–555.
Sandi, C., Haller, J., 2015. Stress and the social brain: behavioural effects and neurobiological mechanisms. Nat. Rev. Neurosci. 16, 290–304.
Schaafsma, S.M., Gagnidze, K., Reyes, A., Norstedt, N., Mansson, K., Francis, K., Pfaff, D.W., 2017. Sex-specific gene-environment interactions underlying ASD-like behaviors. Proc. Natl. Acad. Sci. U. S. A. 114, 1383–1388.
Schaafsma, S.M., Pfaff, D.W., 2014. Etiologies underlying sex differences in Autism Spectrum disorders. Front. Neuroendocrinol. 35, 255–271.
Schindelin, J., Arganda-Carreras, I., Frise, E., Kaynig, V., Longair, M., Pietzsch, T., Preibisch, S., Rueden, C., Saalfeld, S., Schmid, B., Tinevez, J.Y., White, D.J., Hartenstein, V., Eliceiri, K., Tomancak, P., Cardona, A., 2012. Fiji: an open-source platform for biological-image analysis. Nat. Methods 9, 676–682.
Schneider, T., Przewlocki, R., 2005. Behavioral alterations in rats prenatally exposed to valproic acid: animal model of autism. Neuropsychopharmacology 30, 80–89.
Schneider, T., Roman, A., Basta-Kaim, A., Kubera, M., Budziszewska, B., Schneider, K., Przewlocki, R., 2008. Gender-specific behavioral and immunological alterations in an animal model of autism induced by prenatal exposure to valproic acid. Psychoneuroendocrinology 33, 728–740.
Schneider, T., Turczak, J., Przewlocki, R., 2006. Environmental enrichment reverses behavioral alterations in rats prenatally exposed to valproic acid: issues for a therapeutic approach in autism. Neuropsychopharmacology 31, 36–46.
Schwarz, J.M., Bilbo, S.D., 2012. Sex, glia, and development: interactions in health and disease. Horm. Behav. 62, 243–253.
Shi, L., Smith, S.E., Malkova, N., Tse, D., Su, Y., Patterson, P.H., 2009. Activation of the maternal immune system alters cerebellar development in the offspring. Brain Behav. Immun. 23, 116–123.
Sierra, A., Gottfried-Blackmore, A., Milner, T.A., McEwen, B.S., Bulloch, K., 2008. Steroid hormone receptor expression and function in microglia. Glia 56, 659–674.
Spratt, E.G., Nicholas, J.S., Brady, K.T., Carpenter, L.A., Hatcher, C.R., Meekins, K.A., Furlanetto, R.W., Charles, J.M., 2012. Enhanced cortisol response to stress in children in autism. J. Autism Dev. Disord. 42, 75–81.
Vargas, D.L., Nascimbene, C., Krishnan, C., Zimmerman, A.W., Pardo, C.A., 2005. Neuroglial activation and neuroinflammation in the brain of patients with autism. Ann. Neurol. 57, 67–81.
Zablotsky, B., Black, L.I., Maenner, M.J., Schieve, L.A., Blumberg, S.J., 2015. In: Statistics, N.C.f.H (Ed.), Estimated Prevalence of Autism and Other Developmental Disabilities Following Questionnaire Changes in the 2014 National Health Interview Survey, Hyattsville, MD.
Zhan, Y., Paolicelli, R.C., Sforazzini, F., Weinhard, L., Bolasco, G., Pagani, F., Vyssotski, A.L., Bifone, A., Gozzi, A., Ragozzino, D., Gross, C.T., 2014. Deficient neuron-microglia signaling results in impaired functional brain connectivity and social behavior. Nat. Neurosci. 17, 400–406.